

# WIND TURBINE BLADE FAULTS DETECTION

N D Fowkes\*, D P Mason† and J A Teixeira de Freitas‡

## Industry Representative

Adam Mielke§

## Study Group Participants

S Dwyer and M Kalique

### Abstract

De-lamination faults commonly occur in turbine blades either due to faulty manufacturing or as a result of aerodynamic and/or elastic stresses generated during operation. Such faults can dramatically effect the useful life of the turbine. These faults (being sub-surface) are hard to see, let alone detect, even under laboratory conditions. Various detection methods have been suggested including acoustic detection under fatigue blade loading. The MISG was asked to understand and interpret laboratory experiment results obtained using this method.

## 1 Introduction: Turbine Blades

Wind turbines are enormous structures, typically with rotor diameters of 75-100 m supported on poles 100 m high. Turbine blades are specially designed to maximise power output from the turbine and have a distinctive aerodynamic foil shape. Blades are expected to last about 20 years but may last only 4-5 years because of faults formation. The faults are often de-lamination faults which are not easily seen or easy to detect using other means. One procedure for fault detection is using ‘fatigue loading’ with AE (acoustic emission) detection. In this procedure the faults are ‘activated’ by twirling the blade. The faults cause vibrations in the blade which can be measured.

---

\*Mathematics Department, University of Western Australia, Crawley, WA 6009, Australia *email: neville.fowkes@uwa.edu.au*

†School of Computational and Applied Mathematics, University of the Witwatersrand, Johannesburg, South Africa *email: David.Mason@wits.ac.za*

‡Technical University of Lisbon, Instituto Superior Técnico Departamento de Engenharia Civil e Arquitectura, Lisboa, Portugal

§Technical University of Denmark *email: adm@dtu.dk*

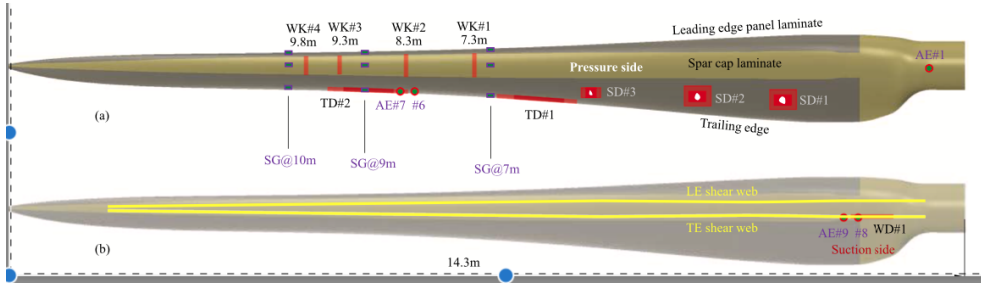


Figure 1: Vertical section through a turbine blade: The blade is relatively ‘thin and flat’ with large surface area, and is strongly tapered.

Adam Mielke from The University of Denmark runs laboratory experiments on 14.3 m long blades with artificially introduced faults. He measures the acoustic response using detectors measuring displacements embedded in the blade, and wants to interpret the results obtained.

This problem was submitted just before the MISG was held so that there was no lead-in time to isolate out a specific question to address at the meeting, and important real data was not presented. Never-the-less the group attempted to determine the nature of the problem, and hopefully our thoughts will be useful; perhaps in a follow-up MISG the issues raised could be addressed. For a very good recent reference for fault detection work in the turbine blades area see [1].

We will first describe the blade structure before going on to discuss the twirling motion used to activate the faults (Section 2). We will then describe the procedure used in the lab to detect the faults (Section 3). The material and structural vibrations excited by faults are of various types and exchanges in energy between these types occur, (Section 4). Unscrambling this response is a difficult matter; some suggestions are made in this section. We conclude with suggestions for further experimental and theoretical work (Section 6).

## 1.1 Blade Shape and Structure

The blade is shaped to be aerodynamically efficient and this requires the leading edge to be blunt, the trailing edge to be sharp, and that the surface area to be as large as possible, given other engineering constraints. The blade tapers off to a tip at the end. The blades are typically 80 m in length and with a typical rotational speed of one revolution in four seconds. This gives a tip speed of 450 km/hr so the associated aerodynamic and elasticodynamic forces acting on the blade are large. The airfoil shape is also such that flaws are likely. Also it should be noted that the detailed shape of the blade (especially its leading edge), as well as surface quality greatly affects the aerodynamic performance (lift and drag) so even minor faults are of concern.

A blade is typically constructed using fibreglass-infused polyester; 30% fibre glass is typical. The main body of the blade is hollow with a sandwich structure near the blade tip (Figure 2). Such structures are usually made by a lamination process. The blade body

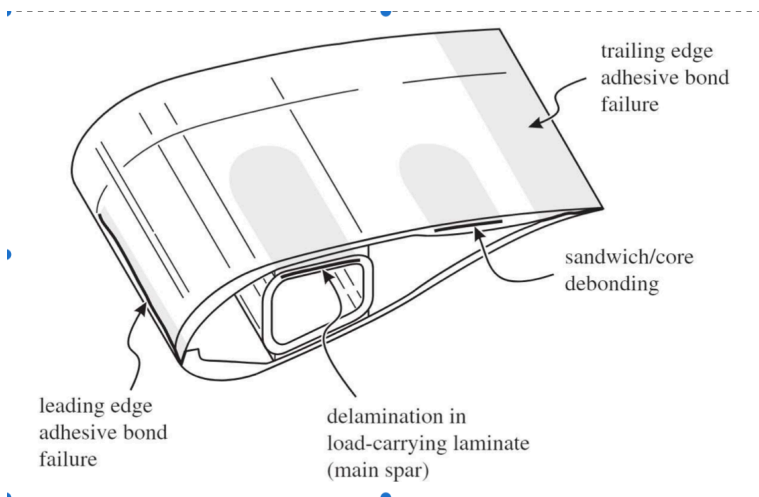


Figure 2: Turbine blade shape and structure. For aerodynamic reasons the leading edge needs to be blunt, the trailing edge needs to be sharp, the upper face convex and the lower face concave. Structural support is needed inside the foil to support the large surface area outside 'skin'. Faults typically occur near the structural support or near the trailing edge.

is either air filled or a light in-fill is used. Usually there are structural supports running down the blade.

Most faults are caused by de-lamination; the adhesive joining layers fails opening up an air filled bubble. A wrinkle may or may not be seen on the surface, so detecting faults is normally difficult. Wrinkles may be formed during construction, and during operation due to blade flexing. Such flexing may cause a wrinkle to form and grow on the blade surface above a de-lamination fault and new wrinkles may appear, see Figure 3. Such faults typically develop near the structural supports (the spar cap), and also near the blade tips, see Figure 4.

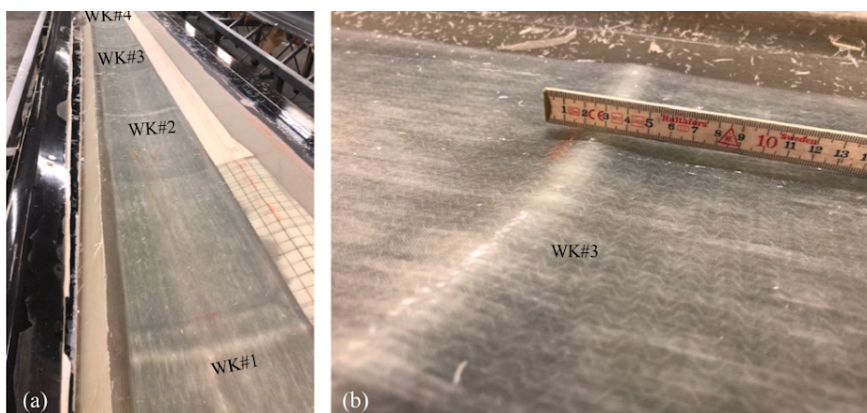


Figure 3: Wrinkles in a turbine blade

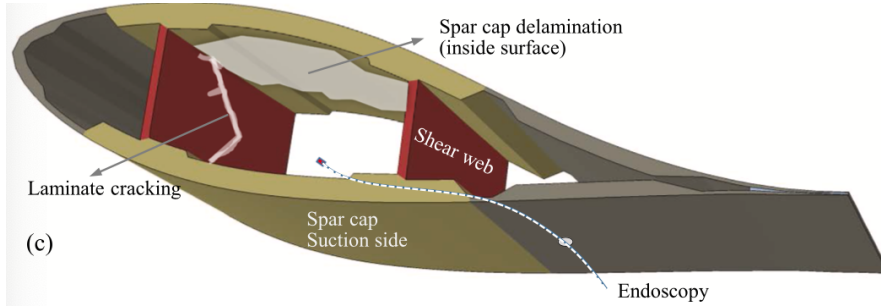


Figure 4: Faults in a blade: Note the de-lamination on the inside of the skin and the structural failure in the strut

## 2 Blade Flexing

The vertical displacement  $y(x, t)$  of a uniform beam is modelled most simply by the Euler-Bernoulli equation [3, 4]

$$EI \frac{\partial^4 y}{\partial x^4} + \rho \frac{\partial^2 y}{\partial t^2} = 0,$$

where  $EI$  is the flexural rigidity of the beam. Our concern is with the ‘flapping mode’ caused by vertically oscillating the base end  $x = 0$  of the beam and with the tip end  $x = L$  free to move; this is the dominant mode of oscillation for the blade. The (forced) boundary conditions at the base end are given by

$$y(0, t) = a \cos \omega t, \quad \frac{\partial y}{\partial x}(0, t) = 0,$$

where  $a$  is the amplitude and  $\omega$  the frequency of the vertical movement, and where it is assumed the end is constrained to remain horizontal. The free end of the beam ( $x=L$ ) has no bending or shear force acting on it which requires [3]

$$\frac{\partial^2 y}{\partial x^2}(L, t) = 0, \quad \frac{\partial^3 y}{\partial x^3}(L, t) = 0.$$

The arrangement used by Adam with the turbine blade in the laboratory corresponds to that described above except in that the base end moves in a vertical plane tracing out a figure eight; again the base end is horizontally constrained and the tip end is free to move. Both vertical (flapping) and span-wise modes are excited in this arrangement, see later.

The forced solution for the beam problem (in scaled form with  $x = Lx'$ ,  $\omega t = t'$ ) is given by

$$y(x', t') = aX(x') \cos t',$$

where

$$X(x') = C_1 \cosh(\lambda x') + C_2 \sinh(\lambda x') + C_3 \sin(\lambda x') + C_4 \cos(\lambda x'),$$

where  $\lambda = J^{-1/4}$ , with

$$J = \frac{EI}{\rho\omega^2 L^4}, \quad (1)$$

and with coefficients  $C_i$  given by

$$\begin{aligned} C_1 &= \frac{1}{2} \left( \frac{1 + \cosh \lambda \cos \lambda + \sin \lambda \sinh \lambda}{1 + \cosh \lambda \cos \lambda} \right), \\ C_2 &= -\frac{1}{2} \left( \frac{\sin \lambda + \cos \lambda \sinh \lambda}{1 + \cosh \lambda \cos \lambda} \right), \\ C_3 &= \frac{1}{2} \left( \frac{\cos \lambda \sinh \lambda + \sin \lambda \cosh \lambda}{1 + \cosh \lambda \cos \lambda} \right), \\ C_4 &= \frac{1}{2} \left( \frac{1 + \cosh \lambda \cos \lambda - \sin \lambda \sinh \lambda}{1 + \cosh \lambda \cos \lambda} \right). \end{aligned}$$

Solution plots are displayed in Figure 5. A resonant response is anticipated by the model when

$$1 + \cosh \lambda \cos \lambda = 0, \quad (2)$$

giving eigenvalues  $\lambda_1 = 1.875$  ( $J = 0.08$ ),  $\lambda_2 = 4.69$  ( $J = 0.002$ ),  $\dots$ .

Note the following:

- It is the value of the dimensionless combination  $J$  that determines the dynamic behaviour of the beam. This means that a small laboratory model can be used to (exactly) determine the dynamic behaviour of a much larger (real scale) beam; the value of  $J$  for the laboratory model just needs to match that of the beam. The dimensionless combination  $J$  varies like  $1/(L^4\omega^2)$  so it is possible to tune a small scale laboratory model to duplicate the behaviour of the larger beam by adjusting  $\omega$ . Note especially that the dynamic behaviour is *very strongly* dependent on beam length. The turbine blade presently used in the laboratory is 14.3 m long; perhaps a smaller model could be used.
- There are a sequence of resonant frequencies; the fundamental (1st) and (2nd) mode are most relevant, see Figure 5. The amplitude of motion increases dramatically as resonance is approached, and near resonance conditions can be effected by changing  $L$  or  $\omega$  with the laboratory scale model. (Of course in practice one would expect a large but finite response under near resonance conditions.) The aim of the laboratory set-up seems to be to ‘fatigue’ the experimental blade so as to stimulate faults (see later). Choosing  $\omega$  so that  $J$  is close to the resonant value for the laboratory  $L$  can achieve a larger amplitude response, and this appears to be what Adam has done in the laboratory. It might be useful in this regard to explore the  $J < 0.08$  range because the shear stress levels generated are much greater if the second flexing mode

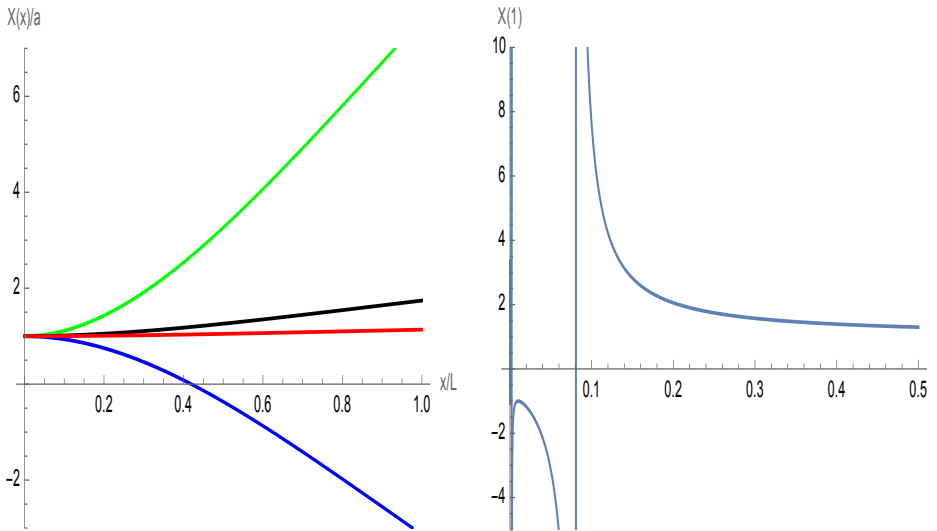


Figure 5: Beam flexing: Left: Curves correspond to the beam displacement when  $t' = \pi/2$  with the base displacement maximal ( $y(0, \pi/2) = 1$ ). Curves are plotted for  $J=0.05$  (blue), 0.1 (green), 0.25 (black), 1.0 (red). Note that the beam will either ‘move in phase with’ the base (black, red, green curves) or in the opposite direction (blue curve) depending on the value of  $J$ . Right: Amplitude of tip end deflection  $X(1)$  as a function of  $J$ . Note  $J = 0.08$  corresponds to the first resonant mode.

is generated; in this mode the two ends of the blade move in opposite directions so that the shear stress levels that most likely cause faults, will be greater. One might also choose  $J$  close to the second resonant value to further enhance the fatigue.

- In the above we have identified  $L$  as being the beam length but vibrations are possible in the cross-beam direction, with the beam width  $W$  replacing  $L$  in the above results. Again there will be resonant frequencies. Importantly, if the proportions  $W/L$  for the laboratory experiment is chosen to match that of the real turbine beam then the behaviour of the two situations will be ‘dynamically similar’; that is one can infer the motion of the full size beam from the smaller laboratory model. Furthermore modal interactions will also correspond, which is very important in context; theoretical models would have to anticipate what interactions matter.
- As indicated earlier turbine blades are of a very special shape and are hollow and internally supported; the beam model is hardly accurate. Never-the-less the qualitative behaviour of the beam model provides useful insight about the behaviour of the turbine blade. As with the beam model there will be a corresponding dimensionless group/s  $J_{eff}$  determining the dynamic behaviour of the turbine blade so that a scaled down laboratory model might be usefully employed to explore the effect of forcing on blade movement. In general terms simple geometric scaling should work but some care will be needed, for example the supporting struts in the laboratory model need to be scaled differently. In any event there will be resonant frequen-

cies associated with flapping and the cross blade modes, which should be measured directly on the real blade and duplicated with the laboratory model; again any theoretical model is likely to have non-obvious inadequacies and so such results are less reliable than actual real world measurements.

- It should be noted that torsional vibrations may also be generated. In fact the modal structure will be strongly dependent on the actual blade structure. The flapping and cross-beam modes described above are likely to dominate but smaller scale features could well be responsible for fault generation. For example faults are observed to occur near the structural support; evidently high stresses are generated near such a support and a local analysis would be needed to study such faults.

## 2.1 Further comments

Adam's experiments do suggest that the experimental turbine blade needs to be moved in a figure eight configuration in order to get 'a fault response'. Such a motion would generate both the longitudinal flapping mode and a cross-blade mode and in fact the energy feed from the (highly energetic) flapping mode to the cross-beam mode is likely to produce high elastic shear stresses near the surface of the blade. (Note that the above beam model does not attempt to model such effects; a modified Timoshenko model[4] would be better, but again the parametric combination  $J$  determines the dominant dynamic behaviour.)

Note also that faults are most likely caused by high frequency modes or transients generated because of a 'mismatch' between blade forcing and natural elastic 'response'; this is a complex problem. It seems likely that design specific features will greatly effect fault generation.

## 3 Fault detection procedure

The ultimate aim of Adam's work seems to be to produce an experimental procedure that would reliably enable engineers to detect a fault in a turbine blade either in a laboratory or under field conditions. In his controlled studies he uses portions of a turbine provided by a supplier. Artificial defects (de-laminations/de-bonding and other) are introduced during (experimental) blade construction. Typically a resin slip foil is inserted between layers during construction, see Figure 3. In between such faults piezoelectric detectors are attached to the surface; (after processing) these measure local displacements as a function of time. The aim is to detect faults and record their growth.

The blade is 'twirled' (about 2 cycles per sec) so that it 'flaps' in the longitudinal direction and oscillates about the blade axis. This complex flexing movement triggers the faults; high frequency ultrasonic *material deformation* stress waves propagate away from the fault (1 kHz or greater). Also incident material deformation waves will be reflected by the fault. This (AE) detection procedure is widely used for fault detection in laminated materials.

Figure 6: Typical displacement response curves recorded in the laboratory

### 3.1 Experimental Results

Results from the detectors needed to be filtered and fitted. The results were in the form of displacements recorded as a function of time at various locations along the laboratory blade. There was insufficient time to examine in detail these results but a good useful description of the process can be found in [2].

## 4 Elastic Waves

The presence of a fault on a moving turbine blade causes material elastic waves to be generated that would not normally be present. We examine the various types of waves that would be generated.

### 4.1 Body Waves

Elastic body deformation waves are of two types: longitudinal/pressure waves (L, P) and transverse/shear (T, S) waves, with **different** wave speeds given by [4] (in engineering parameters)

$$c_L = \sqrt{\frac{E(1-\sigma)}{\rho(1+\sigma)(1-2\sigma)}}, \quad c_T = \sqrt{\frac{E}{2\rho(1+\sigma)}} :$$

$E$  is Young's modulus, and  $\sigma$  Poisson's ratio, or (in scientific parameters)

$$c_L = \sqrt{\frac{\lambda + 2\mu}{\rho}}, \quad c_T = \sqrt{\frac{\mu}{\rho}},$$

where  $\lambda, \mu$  are Lamé coefficients. Note that the waves are non-dispersive and that  $c_L > c_T$ . For materials of interest,  $E=12.0$  GPa,  $\rho = 1.85 \times 10^3$  kg/m<sup>3</sup>, and assuming  $\sigma = 0.3$  we obtain  $c_L = 2.9$  km/sec,  $c_T=1.6$  km/sec; note the difference.

Importantly the nature of an elastic wave is changed when it is reflected or refracted, except under very special circumstances. Thus:

- A monochromatic longitudinal wave passing across an interface between two regions with different propagation properties will transmit a transverse wave as well as a longitudinal wave.
- A monochromatic transverse wave incident on a free boundary (which could be either an external surface or a crack or fault) will generate both reflected longitudinal and transverse waves providing the incidence angle is greater than a critical value. If the incidence angle is exceeds this critical value then a surface wave (a Rayleigh wave) will result, see later.

- A crack (fault) typically propagates ‘with’ (about half) the Rayleigh wave speed.

Surface and bending waves are linear combinations of L and S body waves with the combination determined by the surface conditions.

## 4.2 Surface Waves

Elastic Surface Waves (Rayleigh, Love Waves) may be generated when a body wave hits a surface or a crack (a fault). (The incidence angle needs to be greater than the critical angle.) The wave travels along the surface with speed of approximately  $0.9 c_T$  ([4] p 97), which gives for our materials 1.45 km/sec.

Importantly surfaces (including cracks/faults) can ‘trap’ waves so that much of the elastic energy propagates along the surface.

## 4.3 Bending Waves

Bending waves cause motion at right angles to the surface of beams/rods/plates. They are dispersive and travel with a speed dependent on the ‘plate’ thickness  $h$  as well as the wave number  $k$  [4] p101:

$$c_b = (kh) \sqrt{\frac{E}{3\rho(1 - \sigma^2)}}$$

Notably these waves are anomalous in that shorter waves travel faster than longer waves; an unusual situation which is important in context. For our materials and blades  $kh = \pi$  which gives the wave speed as approximately 4.6 m/sec.

## 5 Observations in Context

- As indicated earlier the body wave composition of an incident wave will change when the wave hits a fault and the resulting wave/s will travel with different speed/s, making detection possible. The received displacement signal will be modulated with its frequency spectrum changed.
- It is likely that surface waves will be generated at a fault so there will be some energy focusing along the fault.
- Shear waves are likely to be highly damped especially because of the composite structure, so detection will be difficult, as indicated by the experimental results.
- The twirling of the blade is likely to result in intermittent wave ‘pulses’ rather than a continuous signal; the observations above are still relevant.

## 5.1 Speculation

The low frequency, large wave length blade swirling just serves to generate material deformation waves of much higher frequency and small wavelength which either cause fault formation or fault ‘stimulation’. Once formed such faults will slip under excitation thus releasing further elastic energy in the form of propagating elastic waves. It is these waves that are detected.

The waves generated by interaction with the fault will be a different combination of the body waves, propagating with different speed so that there will be changed displacement response as recorded by the detectors.

## 6 Conclusions and Suggestions

- This is an important problem and is academically challenging.
- Plastics and composites do not behave like ‘pure linear elastic materials’. Most importantly they are generally ‘lossy’ so, frankly, it seems very unlikely that fault detection using elastic waves would work except over small distances, as evidenced by experimental results.
- Experiments need to be performed on blades without faults; a datum is needed.
- Much more would be needed to be known concerning the material properties and structure of the blades of interest to proceed further.
- There are too many unknowns here: the blade forcing used is really complex, so it is virtually impossible/not practical to determine either the strength location or timing of the source.
- We would guess that the advantage of the present procedure is that it mimics reality but unscrambling the interacting physics is too hard. Even with exact theoretical results this would be impossible; the results are too sensitive to the configuration. It would be useful from the science point of view to set up a simpler experimental configuration (smaller, less expensive, with simpler forcing) to explore the effect of faults in isolation.
- In general terms the problem posed by Adam appears to be primarily a ‘materials problem’, rather than a turbine blade problem. If this is the case then simple experiments could be performed on short strips of the material forming the skin of the blade with introduced faults. The effect of a fault on a propagating wave from a source at the end of the strip could be determined under a variety of conditions (fault location, size, orientation.
- A great deal more time and group/Adam interaction would be required to do this problem justice.

A somewhat analogous situation arises in the geological context, where sound waves are used to detect the possible presence of a mineral deposit. In this case the energy source is known in strength and location and the approximate geometry of the deposit may be known.

In the fault detection situation of Adam's blade experiment the main problem is that the location and size of the energy source is unknown and the response brought about by the fault is strongly dependent on the orientation of the fault, the presence of nearby surfaces etc. This suggests that the best one can do is to check out the frequency spectrum and see if fits in with what is observed in the laboratory for a range of fault orientations. Sophisticated techniques have been developed to handle such time series results. In essence these procedures fit the data using an underlying oscillator/s description.

## References

- [1] McGugan, M., Pereira, G, Sorensen, B. F., Toftegaard, H. and K. Branner, "Damage tolerance and structural monitoring for wind turbine blades", *Phil. Trans. Royal Soc., A*, 373, 2015, pp 1–16.
- [2] Chen, X., Semenov, S., McGugan, M., Madsen, S. H., Yeniceli, S. C., Berring, P., and K. Branner "Fatigue testing of a 14.3 m composite blade embedded with artificial defects Damage growth and structural health monitoring", *Composites: Part A* 140, 2021, pp 1-17.
- [3] Segel, L.A. and Handelman, G. H. "Mathematics Applied to Continuum Mechanics", Fourth Edition, Blackwell Publishing, 2007, pp 193-219.
- [4] Landau, L. D. and Lifshitz, E. M. "Theory of Elasticity", Third Edition, *Course of Theoretical Physics Vol 7*, Pergamon Press, Oxford, 1989, pp 87-104.